

Porous Germanium Layers by Electrochemical Etching for Layer Transfer Processes of High-Efficiency Multi-Junction Solar Cells

E. Garralaga Rojas^a, J. Hensen^a, J. Carstensen^b, H. Föll^b, and R. Brendel^a

^a Institute for Solar Energy Research Hamelin (ISFH), Am Ohrberg 1, D-31860, Emmerthal, Germany

^b Chair for General Materials Science, Faculty of Engineering, Christian-Albrechts-University of Kiel, Kaiserstr. 2, D-24143 Kiel, Germany

We demonstrate reproducible formation of mesoporous germanium layers suitable for solar energy applications by electrochemical etching in highly concentrated electrolytes. For long anodization times or thick layer formation a porosity gradient is observed leading eventually to high porosity regions and cavity formation at the bottom of the porous layer. A 30 min annealing step at a temperature of 575 °C in hydrogen atmosphere allows for reorganization and subsequent lift-off. The mean surface roughness increases from 0.31 nm for unprocessed Ge up to 7.85 nm for reorganized Ge as measured by atomic force microscopy. μ -Raman confocal spectroscopy analysis confirms that etching and annealing do not affect the crystalline structure.

Introduction

Material and cost reduction of III-V compound semiconductors is an important issue for the fabrication of space and concentrator solar cells. Standard III-V multi-junction solar cells are grown by Chemical Vapour Deposition (CVD) on germanium substrate wafers. After first epitaxial growth, the function of the substrate is reduced to being the bottom cell in the stack and an expensive carrier providing mechanical stability during cell processing. The thickness of the Ge wafer typically exceeds 100 μm , whereas 2-6 microns would be sufficient for the bottom cell to match the photogenerated currents at the top and middle solar cells. Thick substrates hence increase weight and costs for concentrator systems and reduce the payload for satellite missions.

Reduction of unnecessary weight is compulsory in order to optimize the power-to-mass ratio of multi-junction solar cells. Ge substrates are thus commonly dissolved in a chemical wet solution or cut-off with a saw. This technique permits the fabrication of ultra-thin solar cells but the (expensive) Ge substrates are lost for further use. Lift-off processes based on porous layers could solve the problem by separating the active layer from the substrate and allowing re-use of the substrate. Brendel demonstrated the so-called Porous Silicon Process (PSI Process) for the fabrication of highly-efficient thin-film monocrystalline solar cells (1). This method uses a porous Si double layer formed by means of electrochemical etching. A mesoporous layer with low porosity at the surface of the substrate is used as a seed layer for the Si epitaxy, while a buried high porosity layer is used as a pre-structured separation plane.

Whereas porous Si formation is well studied, porous Germanium (PGe) has not been intensively investigated. Choi and Buriak first produced PGe by changing once the etching bias from anodic to cathodic. HCl was used as electrolyte with a concentration of 70 wt. % and very high etching current densities around 300 mAcm^{-2} were applied (2).

Flamand *et al.* from IMEC in Belgium studied PGe formation for a lift-off process (3), using HF as electrolyte. They obtained macropores, etch pits, and a porous film that was not mechanically stable. Lift-off was not possible under such etching conditions. The Christian-Albrechts-University of Kiel investigated pore formation in Germanium by electrochemical etching extensively, focusing mostly on macropore and nanowire formation (4)-(8). Langa *et al.* showed that PGe formation is always accompanied by a constant dissolution of the already-formed pores (4),(5). We have demonstrated the formation of single and multi-layers by electrochemical etching in highly concentrated HF-based electrolytes (9)-(11). The dissolution of the already-formed porous layer is avoided by alternating the etching bias from anodic to cathodic (9), thus allowing double- and multi-layer formation. We recently investigated porosity and reorganization of the porous layers under different annealing and atmospheres (12). Reorganization strongly depends on the porosity: Porous layers with porosities below 30 % get compacted and show a closed surface whereas porous layers with porosities exceeding 50 % collapse and behave similarly to separation layers in the PSI process.

In this paper, we experimentally demonstrate etching and lift-off of porous Ge layers with a gradient in the porosity and cavity formation at the bottom of the porous layers. The gradient in the porosity is obtained by applying long etching durations or preparing thick porous layers. A hydrogen annealing step permits porous reorganization and subsequent layer transfer.

Experimental

Germanium wafers with a thickness of (150 ± 10) μm serve for electrochemical etching experiments. The substrates are p-type and one-side polished. The orientation is $\{100\}$ with a miscut of 6° towards $\{111\}$ and the specific resistivity is (25 ± 15) $\text{m}\Omega\text{cm}$. A double-container etching cell made from highly acid resistant polypropylene is used for electrochemical etching and porous layer formation of Ge. The electrolyte is aqueous hydrofluoric acid (HF) with a concentration varying in a range of 30-50 wt. %. The potentiostat Elypor 3 (ET&TE Etch & Technology GmbH) allows different etching profiles in either galvanostatic or potentiostatic mode and in anodic or cathodic bias conditions. After anodizing, samples are rinsed in de-ionized water and dried under N_2 stream. The layers' porosity is calculated by gravimetric measurements in reference PGe samples.

A LPT Serius Lab 100 furnace serves for sample annealing in hydrogen atmosphere. The oven tube is flushed for 30 min prior to annealing with a gas flow of 30 l min^{-1} in order to remove residual oxygen. The temperature is 575°C and the hydrogen gas flow is set to 15 L min^{-1} during annealing. The total duration is 60 min with a 15 min plateau at the nominal temperature.

The morphology and thicknesses of the porous layers are inspected in a high resolution Hitachi S-4800 Scanning Electron Microscope (SEM). Electron Dispersive X-ray analysis (EDX) is used for material investigation. Surface roughness is investigated using a multi-mode Atomic Force Microscope (AFM, Digital Instruments, Nanoscope III controller). μ -Raman confocal spectroscopy serves for structural analysis.

Results and discussion

The porosity of a layer is defined as the ratio of the volume of all the pores in a layer to the volume of the layer without pores. The porosity is a key parameter, as it determines thermal reorganization of the porous layer during the annealing step. We studied the dependence of the porosity on several parameters such as specific resistivity of the substrate, etching current density, and electrolyte concentration (10),(12). In the case of mesoporous germanium, the porosity decreases with increasing substrate specific resistivity and electrolyte concentration and with decreasing etching current density.

Figure 1 shows the SEM cross section image of a mesoporous germanium layer. Aqueous hydrofluoric acid with a concentration of 50 wt. % serves as electrolyte. The etching current density is set to 10 mA cm^{-2} and the etching time is 1 hour. The specific resistivity of the substrate is $22 \text{ m}\Omega\text{cm}$.

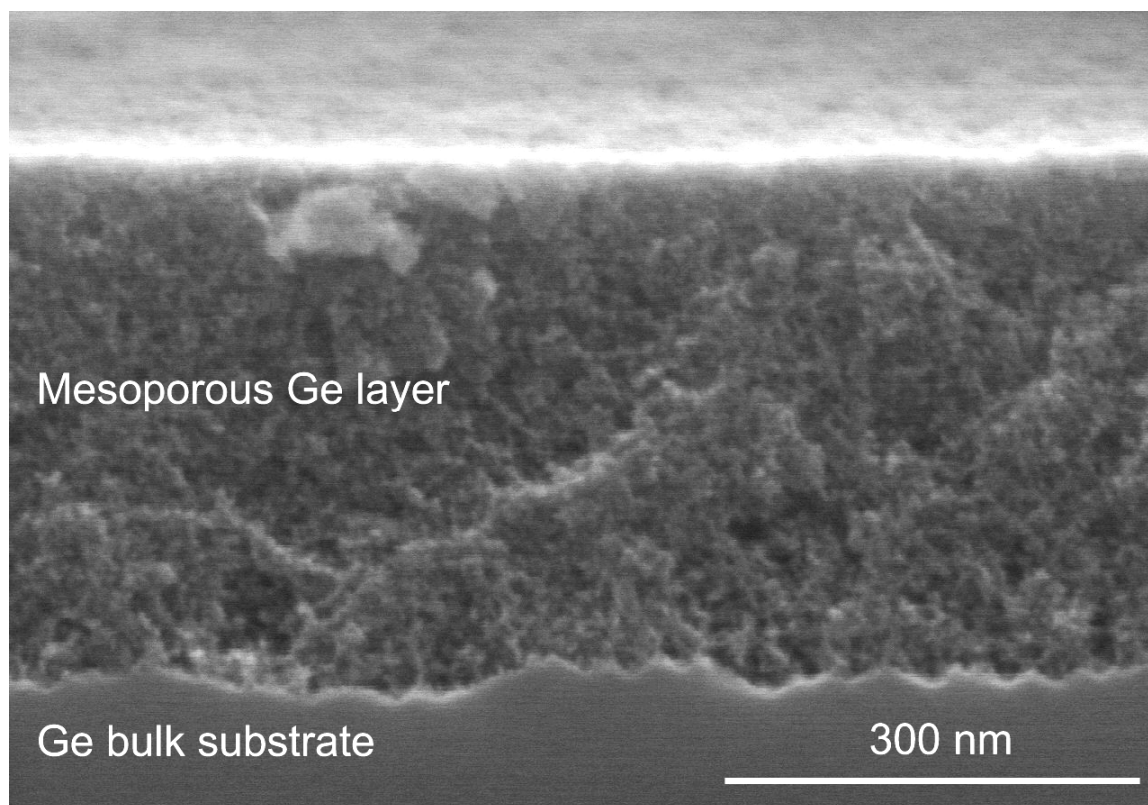


Figure 1. Mesoporous Ge layer with homogeneous porosity distribution.

The sample shown in Figure 1 has a thickness of $390 \pm 15 \text{ nm}$. The diameter of the pores lies in a range of 1 nm to 40 nm and the mean diameter of the pores is 12.4 nm as measured with imaging recognition software. The porosity is $52 \pm 4 \%$ and it is homogeneous over the porous layer volume.

A homogeneous distribution of the porosity is only correct for short anodization times and thin porous layers. We observe that the porosity is not homogeneously distributed in layers with increasing etching duration (over 10 hours) or with a porous layer thickness exceeding 900 nm. HF concentration and renewal of fluorine atoms decrease due to diffusion limitations at the bottom of the porous layer. The porosity therefore increases with pore depths and time consuming experiments. As a consequence, the porosity presents a gradient in the porosity within the porous layer with a peak at the bottom of the porous layer. This effect has also been reported in silicon (13). In case of very long

electrochemical etching experiments with very low etching current densities, the increase in the porosity drives in extreme cases to cavity formation as shown in Figure 2.

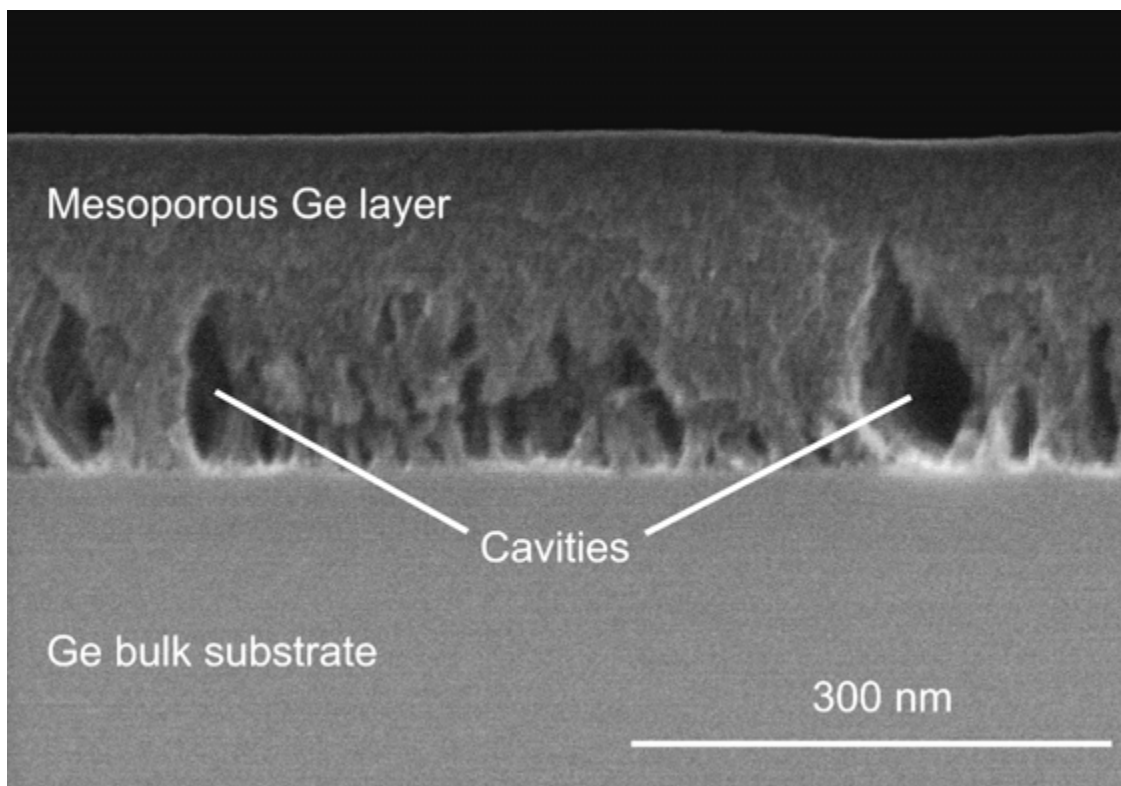


Figure 2. SEM cross-section of mesoporous Ge etched 22 hours in HF 50 wt. % with an etching current density of 0.5 mA cm^{-2} . The bottom of the porous layer presents an increased porosity caused by lower HF concentrations that leads to large cavity formation.

Figure 3 shows the cross section of a reorganized PGe layer with varying porosity throughout the layer. The porous layer was etched 15 hours in HF 50 wt. % with an etching current density of 1 mA cm^{-2} . The substrate resistivity is $20 \text{ m}\Omega\text{cm}$. H_2 -atmosphere serves for annealing 30 min at $575 \text{ }^\circ\text{C}$.

Annealing of porosity-graded layers causes the upper part of the porous layer to become closed and compacted. Figure 3.a shows a SEM cross-section of a reorganized PGe layer. The lower part of the layer automatically detaches from the substrate due to increased porosity and the presence of large cavities at the bottom of the porous layer. Layer transfer is hence possible by adhering a sticky pad to the PGe layer as shown in Figure 3.b. EDX analysis confirms the presence of transferred PGe layer to the sticky pad. Figure 3.c shows the backside of the sticky pad and Figure 3.d shows the marks of previous layer transfer experiments.

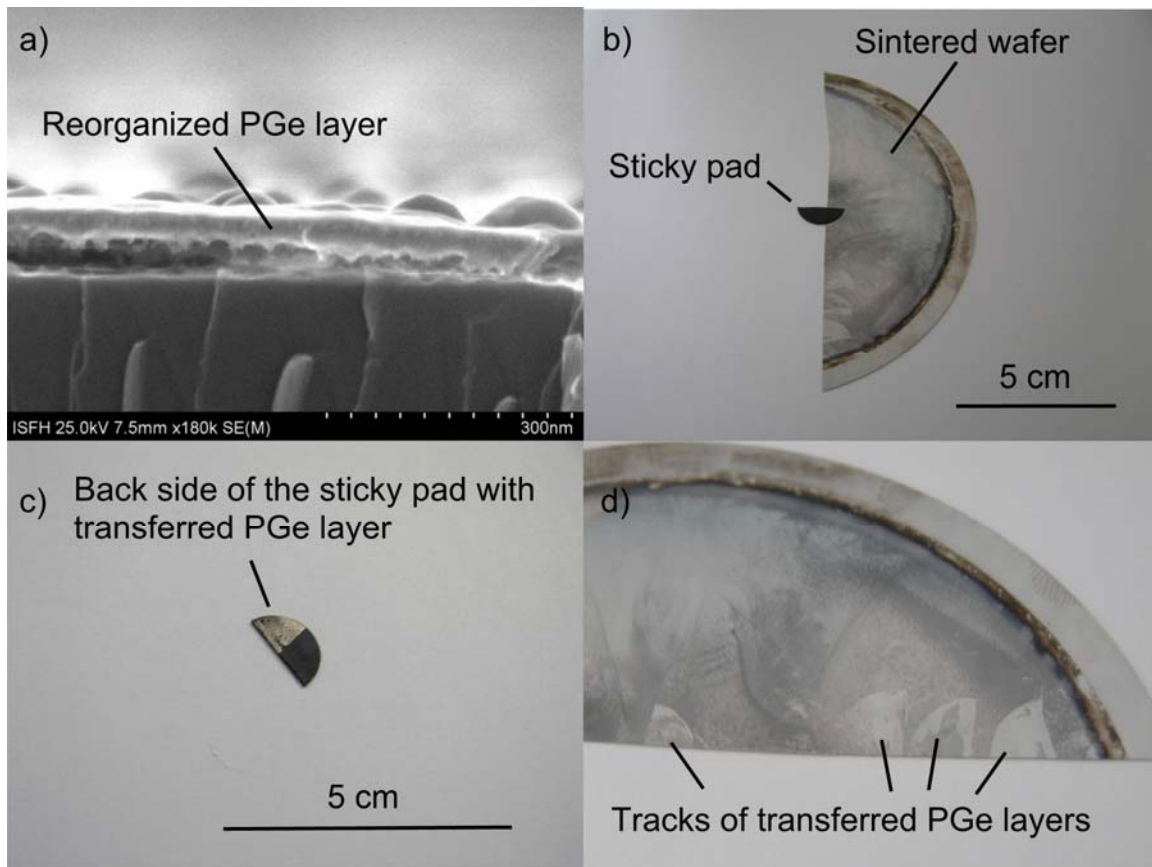


Figure 3. Figure a) shows a SEM caption of the reorganized PGe layer after annealing. The reorganized layer detaches from the substrate automatically. Figure b) shows a sticky pad adhered to the half of a sintered wafer. In Figure c), the backside of the sticky pad shows the transferred PGe layer. Finally, Figure d) shows the marks of previous layer transfer experiments.

μ -Raman confocal spectroscopy serves for structural analysis of PGe layers. Figure 4 shows a μ -Raman shift analysis of a PGe layer. The black solid line refers to a blank reference wafer without PGe layer. The dotted red line refers to a PGe etched layer and the green dashed line refers to a sintered and reorganized PGe layer. Independently of the intensity, no Raman shift is observable and all three peaks lie at the same value of 300 cm^{-1} , which is the characteristic Ge I-peak and has been already observed in the literature for Ge bulk substrates (14). This measurement confirms that etching and annealing of PGe do not affect the crystalline structure of the substrate and remains monocrystalline after reorganization.

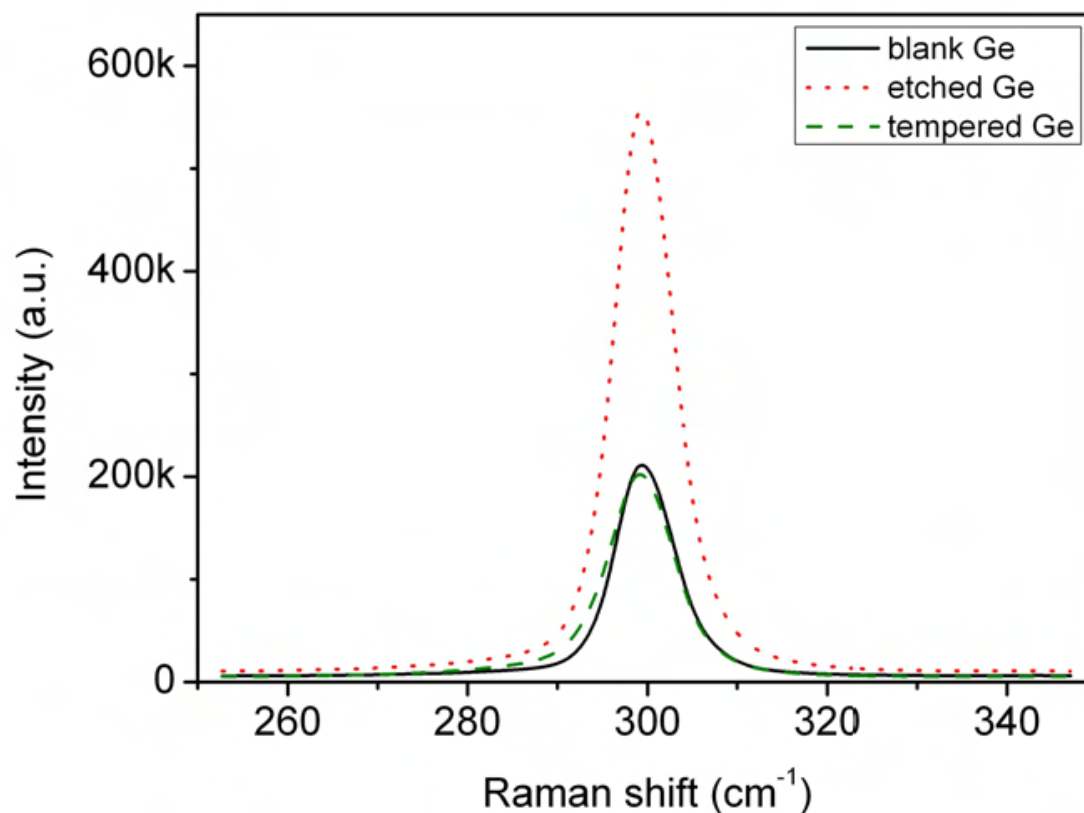


Figure 4. Detailed μ -Raman shift analysis of mesoporous Ge. No shift is observable and all three peaks center at 300 cm^{-1} .

Surface roughness is an important parameter for a subsequent epitaxy of III-V compounds. AFM analysis serves for surface characterization and roughness measurements. Figure 5 shows AFM 3-D scan micrographs with a size of $2 \times 2\ \mu\text{m}$ for each step of the PSI process: Ge bulk substrates, as-etched substrates, and reorganized and closed PGe layers in hydrogen atmospheres. Figure 5.a shows the surface of unprocessed Ge. The maximum peak-valley height difference, i.e. the height difference between the highest and the deepest point of the surface, is $2.13 \pm 0.1\ \text{nm}$. The average surface roughness is $0.31 \pm 0.1\ \text{nm}$. Figure 5.b shows a mapping of the surface of a Ge wafer after electrochemical etching. The maximum height difference is $21.66 \pm 0.1\ \text{nm}$ and the mean surface roughness is $3.52 \pm 0.1\ \text{nm}$. Figure 5.c shows the surface of PGe after etching and annealing in hydrogen atmosphere 15 min at $600\ ^\circ\text{C}$. The maximum height difference is $44.94 \pm 0.1\ \text{nm}$ and the average surface roughness is $7.85 \pm 0.1\ \text{nm}$.

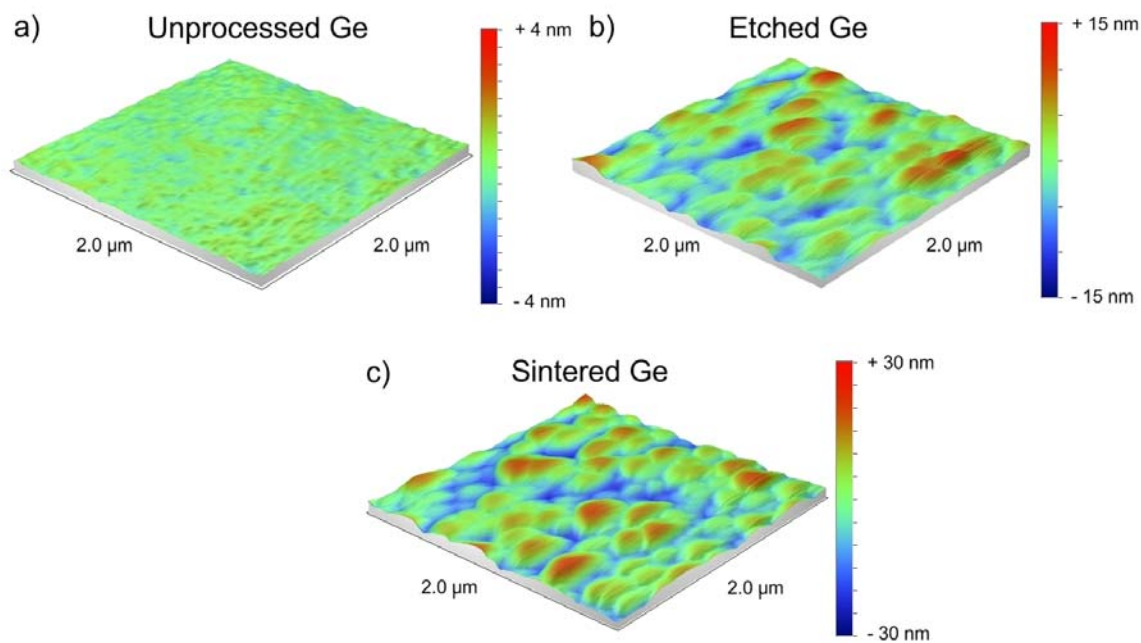


Figure 5. AFM 3-D scan micrographs of the surface of a) Ge blank wafer, b) Etched PGe wafer, and c) Reorganized PGe wafer in hydrogen atmosphere. Note that each measurement has a different height scale.

Figure 5.a shows an unprocessed Ge wafer that has a flat surface appropriate for epitaxy. Figure 5.b shows the surface of an etched PGe wafer. The increased surface roughness is caused by strong electropolishing of the already formed porous layer. Substrate reorganization in hydrogen atmosphere yields a compacted layer with higher substrate roughness as in the etched state. Further experiments will investigate whether this substrate roughness is sufficient for epitaxial growth.

Summary

We demonstrate reproducible lift-off of reorganized PGe layers produced by electrochemical etching. Long etching experiments (> 10 hours) or thick porous layers (> 900 nm) lead to a porosity gradient with a peak at the bottom of the layer. HF concentration and renewal of fluorine atoms decrease due to diffusion limitations at the bottom of the porous layer, hence influencing the porosity. The gradient allows for different reorganization at the upper and lower part of the porous layer in a subsequent annealing step in hydrogen atmosphere. The porous layer surface closes during annealing whereas the lower part increases its volume, separates, and allows lift-off. μ -Raman confocal spectroscopy shows that neither etching nor annealing in hydrogen affect the crystallinity. AFM measurements show an increase in the mean surface roughness from 0.31 nm to 7.85 nm. Further research will concentrate on reducing surface roughness and investigate whether epitaxial growth is possible on removable PGe layers.

Acknowledgments

The authors would like to thank Daniel Tutuc and Prof. Rolf Haug from the University of Hannover for the AFM measurements, V. Wiedemeier and G. Berth from the University Paderborn for the μ -Raman measurements, and Bianca Gehring from the ISFH for the technical assistance. The financial support of this work by the German Ministry for Economy and Technology under contract No. 50JR0641 is gratefully acknowledged. E. Garralaga Rojas specially thanks the European Space Agency for the financial support of his work in the framework of the Networking Partnering Initiative (Co. No. 20250/06/NL/GLC).

References

1. R. Brendel, in *Proc. of the 14th EUPVSEC*, Barcelona, (1997), pp. 1354-1357.
2. H.C. Choi and J. Buriak, *Chem. Comm.*, pp. 1669-1670, (2000).
3. G. Flamand, J. Poortmans, and K. Dessein, *Phys. Stat. Sol. (C)* **2**, No. 9, pp. 3243-3247, (2005).
4. S. Langa, M. Christophersen, J. Carstensen, I. M. Tiginyanu, and H. Föll, *Phys. Stat. Sol. (A)* **195**, pp. R4-R6 (2003).
5. S. Langa, J. Carstensen, M. Christophersen, K. Steen, S. Frey, I. M. Tiginyanu, and H. Föll, *J. Electrochem. Soc.* **152**, (8) pp. C525-C531 (2005).
6. S. Langa, J. Carstensen, I. M. Tiginyanu, and H. Föll, *Phys. Stat. Sol. (C)* **2**, No. 9, pp. 3237-3242 (2005).
7. C. Fang, H. Föll, and J. Carstensen, *J. Electroanal. Chem.* **589**, pp. 259-288, (2006).
8. C. Fang, H. Föll, J. Carstensen, and S. Langa, *Phys. Stat. Sol. (A)* **204**, No. 5, pp. 1292-1296 (2007).
9. E. Garralaga Rojas, H. Plagwitz, B. Terheiden, J. Hensen, C. Baur, G. La Roche, G. Strobl, and R. Brendel, *J. Electrochem. Soc.* **156**, 8, pp. D310-D313 (2009).
10. E. Garralaga Rojas, B. Terheiden, H. Plagwitz, J. Hensen, C. Baur, G. Strobl, and R. Brendel, *Electrochem. Comm.* **12**, 2, pp. 231-233 (2010).
11. E. Garralaga Rojas, J. Hensen, J. Carstensen, H. Föll, and R. Brendel, *Phys. Stat. Sol. (C)* (2010), accepted for publication.
12. E. Garralaga Rojas, J. Hensen, C. Baur, and R. Brendel, *Sol. Energy Mater. Sol. Cells* **95**, pp. 292-295 (2011).
13. V. Lehmann, *Electrochemistry of Silicon*, Wiley-VCH Verlag GmbH, Weinheim, Germany (2002).
14. S. Wen, J. Jan, M. Lance, J. Bentley, and G. Pharr, *Microsc. Microanal.* **11**, 2, pp. 792-793 (2005).